Original Research

SLAS Discovery
2020, Vol. 25(8) 906–922

DOI: 10.1177/2472555220918367
journals.sagepub.com/home/jbx
SAGE

HTS-Compatible CometChip Enables Genetic Screening for Modulators of Apoptosis and DNA Double-Strand Break Repair

Ian J. Tay[1,2,3], James J. H. Park[4], Anna L. Price[4], Bevin P. Engelward[1*], and Scott R. Floyd[4,5*]

Abstract

Dysfunction of apoptosis and DNA damage response pathways often drive cancer, and so a better understanding of these pathways can contribute to new cancer therapeutic strategies. Diverse discovery approaches have identified many apoptosis regulators, DNA damage response, and DNA damage repair proteins; however, many of these approaches rely on indirect detection of DNA damage. Here, we describe a novel discovery platform based on the comet assay that leverages previous technical advances in assay precision by incorporating high-throughput robotics. The high-throughput screening (HTS) CometChip is the first high-throughput-compatible assay that can directly detect physical damage in DNA. We focused on DNA double-strand breaks (DSBs) and utilized our HTS CometChip technology to perform a first-of-its-kind screen using an shRNA library targeting 2564 cancer-relevant genes. Conditions of the assay enable detection of DNA fragmentation from both exogenous (ionizing radiation) and endogenous (apoptosis) sources. Using this approach, we identified LATS2 as a novel DNA repair factor as well as a modulator of apoptosis. We conclude that the HTS CometChip is an effective assay for HTS to identify modulators of physical DNA damage and repair.

Keywords

high-throughput screening, RNA interference, Comet assay, DNA double-strand breaks, ionizing radiation, LATS2, Hippo pathway, nonhomologous end joining, homologous recombination

Introduction

Maintenance of DNA integrity is crucial for high-fidelity transmission of genetic information to progeny cells. Threats to DNA integrity can be cell-extrinsic (e.g., ionizing radiation, chemicals) and/or cell-intrinsic (e.g., metabolites, apoptosis induced). DNA damage can also interfere with critical cellular processes and lead to cancer-causing changes in the genome.[1,2] DNA double-strand breaks (DSBs) in particular can have severe consequences as part of the apoptotic program, by causing genomic alterations that cause loss or dysfunction of genetic information, or by triggering cell death via DNA damage signaling.[3] DNA repair pathways safeguard the genome against the deleterious effects of DNA DSBs, and dysregulated DNA repair is often observed in pathological conditions such as cancer.[2] Likewise, apoptosis is highly regulated in normal cells, and dysregulation is a hallmark of cancer.[2] While defective DNA repair can destabilize the genome, thus promoting cancer, these same defects can render cancer cells vulnerable to DNA damage in the

[1]Department of Biological Engineering, Center for Environmental Health Sciences, Massachusetts Institute of Technology, Cambridge, MA, USA
[2]Agency of Science, Technology and Research Graduate Academy, A*STAR Singapore, Singapore
[3]Institute of Molecular and Cellular Biology, A*STAR Singapore, Singapore
[4]Department of Radiation Oncology, Duke University School of Medicine, Durham, NC, USA
[5]Koch Institute for Integrative Cancer Research, Cambridge, MA, USA
*These authors contributed equally.

Received Sept 11, 2019, and in revised form March 1, 2020. Accepted for publication March 3, 2020.

Supplemental material is available online with this article.

Corresponding Author:
Bevin P. Engelward, Department of Biological Engineering, Center for Environmental Health Sciences, Massachusetts Institute of Technology, 77 Mass. Ave. 16-743, Cambridge, MA 02139, USA.
Email: bevin@mit.edu

form of radio- or chemotherapy. Therefore, a better understanding of DNA repair and apoptosis pathways can lead to improved cancer therapy. Here, we describe an advance in the throughput of physical DNA DSB detection using a platform that is designed to be compatible with high-throughput screening (HTS) technologies. We leveraged this novel approach for gene discovery to further our understanding of DNA DSB repair and apoptotic pathways.

DSBs are repaired via two major pathways in human cells, namely, homologous recombination (HR) and nonhomologous end joining (NHEJ).[4] In the HR pathway, the broken DNA strands are end resected to create 3′ overhangs that invade homologous DNA on sister chromatids to copy genetic information for repairing the break.[5] Due to the requirement of sister chromatids as a source of template DNA for accurate repair, the HR pathway is generally most active during the S and G_2 phases of the cell cycle.[6] In contrast, NHEJ does not require a homologous template, and therefore is active throughout the cell cycle.[7] For NHEJ, broken ends of DNA strands are protected from end resection by the Ku70/Ku80 heterodimer, effectively inhibiting HR.[8] DNAPKcs then binds to the Ku70/Ku80 heterodimers at the DNA DSB to form the DNAPK holoenzyme.[9] Upon activation, DNAPK is able to phosphorylate itself, as well as many downstream NHEJ factors, including the Artemis protein,[10] which is one of the major end processing endonucleases recruited to DSBs with nonligatable ends. Other end processing enzymes recruited to DSBs include PNKP,[11] which removes phosphate groups from 3′ ends and phosphorylates hydroxyl groups on 5′ ends, as well as DNA polymerases Pol μ and λ.[12] The broken DNA ends are then ligated together by a complex composed of XRCC4, XLF, PAXX, and DNA ligase IV.[13,14] These key components of the HR and NHEJ pathways are critical for efficient DSB repair, and loss of function of these genes leads to persistent DSB following DNA damage.

Given that genes that modulate DNA repair could be useful targets for novel cancer therapeutics, many laboratories have screened for genes directly involved in DSB repair and for genes that indirectly impact DSB repair (e.g., genes involved in chromatin remodeling or cell signaling). For example, proximity ligation approaches coupled to mass spectrometry proteomics have revealed entire networks of proteins that associate at sites of DNA damage.[15] In addition, researchers have employed knockdown or knockout libraries to screen thousands of genes for their ability to modulate DNA damage responses. Such responses have included co-localization of proteins involved in DNA DSB responses (e.g., γH2AX, 53BP1, and Rad52), as well as synthetic lethality (e.g., sensitization of BRCA2 mutant cells). Using these methods, networks of interacting genes that modulate DNA DSB levels have been revealed, as well as specific genes that participate in DNA DSB recognition and repair.[16,17] These studies have shown the utility of large-scale genomic screening to identify novel DNA repair genes that could lead to novel strategies for treating cancer. However, none of these large-scale studies exploit methods to directly measure the levels of physical DNA DSBs in cells. For example, downstream signaling events (such as phosphorylation of H2AX) or changes in protein co-localization are associated with, but do not occur exclusively in the presence of, DNA DSBs. In addition, cell survival and synthetic lethality assays rely on lethal interactions that may or may not be due to changes in DSB repair. We therefore set out to perform a large-scale RNAi screen using detection of physical DNA DSBs as an approach to identify previously unknown genes that impact DNA damage formation and repair.

The comet assay is a well-established assay for DNA DSBs[18] directly induced by DNA-damaging agents (e.g., ionizing radiation) or indirectly induced as a result of enzymatic DNA fragmentation that occurs during apoptosis.[19,20] The comet assay technique, first described by Ostling and Johanson in 1984 and further developed by many others,[21–24] is based on the principle that damaged DNA has greater electrophoretic mobility in an agarose gel compared with intact DNA, resulting in a comet-shaped distribution of DNA within the gel (where a nucleoid forms the head and damaged DNA forms the tail). Traditionally, the assay requires spotting a molten agarose cell suspension onto a glass slide with one condition per slide, and therefore it is extremely low throughput and tedious to perform. Users also report high variation in the results obtained from the assay, preventing its usage in large-scale screens. To address the limitations of the comet assay, Andrew Collins's group[25] and Trevigen, Inc. (Gaithersburg, MD) created slides with subregions, which greatly improved throughput and consistency, but the assay is performed using standard imaging and analysis, which can be quite slow and inconsistent among experimentalists. Wood and coworkers developed the CometChip,[26–28] which also subdivides a glass slide, in this case with 96 regions in the conformation of a 96-well plate. The CometChip also exploits cell micropatterning, which maximizes the number of useful comets per unit area, prevents overlapping comets, creates a uniform focal plane (enabling the use of only one or two images to capture ~100 comets, rather than one image per comet), and enables automated imaging and analysis (increasing throughput by orders of magnitude). To create a cell array, microfabrication techniques are exploited to create a stamp that can be applied to molten agarose to create an agarose slab with an array of cell-sized microwells. When a cell suspension is placed over the agarose, cells enter the microwells by gravity and are then processed using standard comet assay conditions to create an array of comets. The bed of arrayed microwells can be made to the size of a standard multiwell plate and can be partitioned into 96 compartments by using a bottomless 96-well plate, each with ~300 comets per well.

The approach effectively miniaturizes the assay, enabling conversion from one glass slide per sample (the traditional assay) to one 96-well per sample. With the CometChip, multiple samples can be prepared in parallel on the same assay substrate, and throughput is greatly increased via automated imaging and analysis using either in-house or commercially available software available through Trevigen, Inc. However, the existing hardware for performing the CometChip is not compatible with HTS robotics, because the hardware dimensions do not match a typical multiwell plate, a requirement for automated manipulation of 96-well plates. Here, we describe a novel advance in the throughput of DNA damage detection by creating hardware that conforms to the requirements of high throughput robotics and is compatible with standard automated microscopes. The HTS CometChip enables large-scale screens. We leveraged this platform to perform a large-scale shRNA screen of 2564 human genes wherein the levels of DNA DSBs were directly measured. From the screen, we identified LATS2, as a modulator of both apoptosis and DNA repair. We furthermore show that in addition to its role in regulation of cell–cell contact survival, LATS2 modulates DNA repair and radiation sensitivity. Beyond these new roles for LATS2, this work establishes the utility of the HTS CometChip as a tool for the discovery of novel genes that impact DNA damage and repair.

Materials and Methods

Cell Culture

M059K and M059J human glioblastoma cells from ATCC (Manassas, VA) were cultured in 1:1 DMEM/F12 nutrient mix (Invitrogen-Thermo-Fisher Scientific, Waltham, MA) supplemented with 10% fetal bovine serum (FBS; Atlanta Biologicals, Atlanta, GA), 1× MEM Non-Essential Amino Acids (Invitrogen), and 100 units/mL penicillin-streptomycin (Invitrogen). HeLa human cervical adenocarcinoma cells from ATCC were cultured in DMEM (Invitrogen) supplemented with 10% FBS (Atlanta Biologicals) and 100 units/mL penicillin-streptomycin (Invitrogen).

HTS CometChip Apparatus Fabrication

A 120 × 78 mm aluminum base plate was cut from a 3 mm thick aluminum sheet to fit tightly in a uniwell tray (VWR, Radnor, PA). Four aluminum posts (6 mm in diameter and 6.5 mm in height) were welded onto the base plate with their centers 28.5 mm and 7.5 mm from the short and long edges of the plate, respectively. A 2 mm wide and 5 mm deep hole was drilled parallel to the long axis of each of the posts, from the center of their flat surfaces. The outer edges of a bottomless 96-well plate (VWR) were sawed off, leaving a 110 × 74 mm grid of 96 wells. Wells A3, A10, H3, and H10 were plugged with tight-fitting polystyrene cylinders with a 2 mm wide hole drilled at their centers. HTS CometChip was assembled by sandwiching the microwell arrayed agarose between the aluminum base plate and the bottomless well plate, such that the posts on the aluminum plate meet the pegs on the bottomless plate, and fastening them together with screws.

Neutral CometChip

The standard CometChip was prepared as described previously.[27] Briefly, 12 mL of 1% molten agarose in PBS is poured over a GelBondflim (Lonza, Basel, Switzerland) placed on a uniwell tray (VWR). A reusable PDMS stamp arrayed with 40 µm wide microposts is floated on the molten agarose and the agarose is allowed to cool and solidify. Following gelation, the PDMS stamp is removed to reveal microwells for cell loading. The agarose and the GelBond film are placed on a glass plate, and a bottomless 96-well plate (VWR) is clamped onto the agarose using binder clips to assemble the standard CometChip. The HTS CometChip assembly is described in **Figure 1**. The microwell array is poured on GelBond film and held between the aluminum base plate and a bottomless 96-well plate with four screws. Cell suspensions are loaded into individual wells of the bottomless 96-well plate and the apparatus is placed in a 37 °C incubator for 20 min to allow cell loading. After cell loading of either standard or HTS CometChip, excess cells are washed off with PBS, and a thin layer of 1% molten low-melting-point agarose in PBS is applied on the top surface of the CometChip. Cells within the CometChip are exposed to DNA-damaging agents (e.g., γIR) and placed in complete media for recovery. Cells are then lysed at 43 °C overnight after desired time points by submerging the CometChip into lysis buffer containing 2.5 M NaCl, 100 mM Na_2 EDTA, 10 mM Tris, 1% *N*-lauroylsarcosine, pH 9.5, with 0.5% Triton X-100 and 10% DMSO. After cell lysis, the CometChip is washed three times with neutral electrophoresis buffer containing 90 mM Tris, 90 mM boric acid, 2 mM Na_2 EDTA, pH 8.5. Electrophoresis was conducted using prechilled neutral electrophoresis buffer at 4 °C for 1 h at 0.6 V/cm and 6 mA. The CometChip is then stained with SYBR Gold (Invitrogen) according to the manufacturer's instructions and images are taken using an upright fluorescent microscope with a 4× objective for non-high-throughput experiments (https://zenodo.org/record/2656668#.XqhZ6GhKhaQ). Comets are analyzed for the lengths of their tail region using a custom-made script written in MatLab (MathWorks, Natick, MA): the code is available from DOI: 10.5281/zenodo.2656668.

HTS Robotics

Access to HTS robotics and equipment was obtained via MIT's Koch Institute of Integrative Cancer Research,

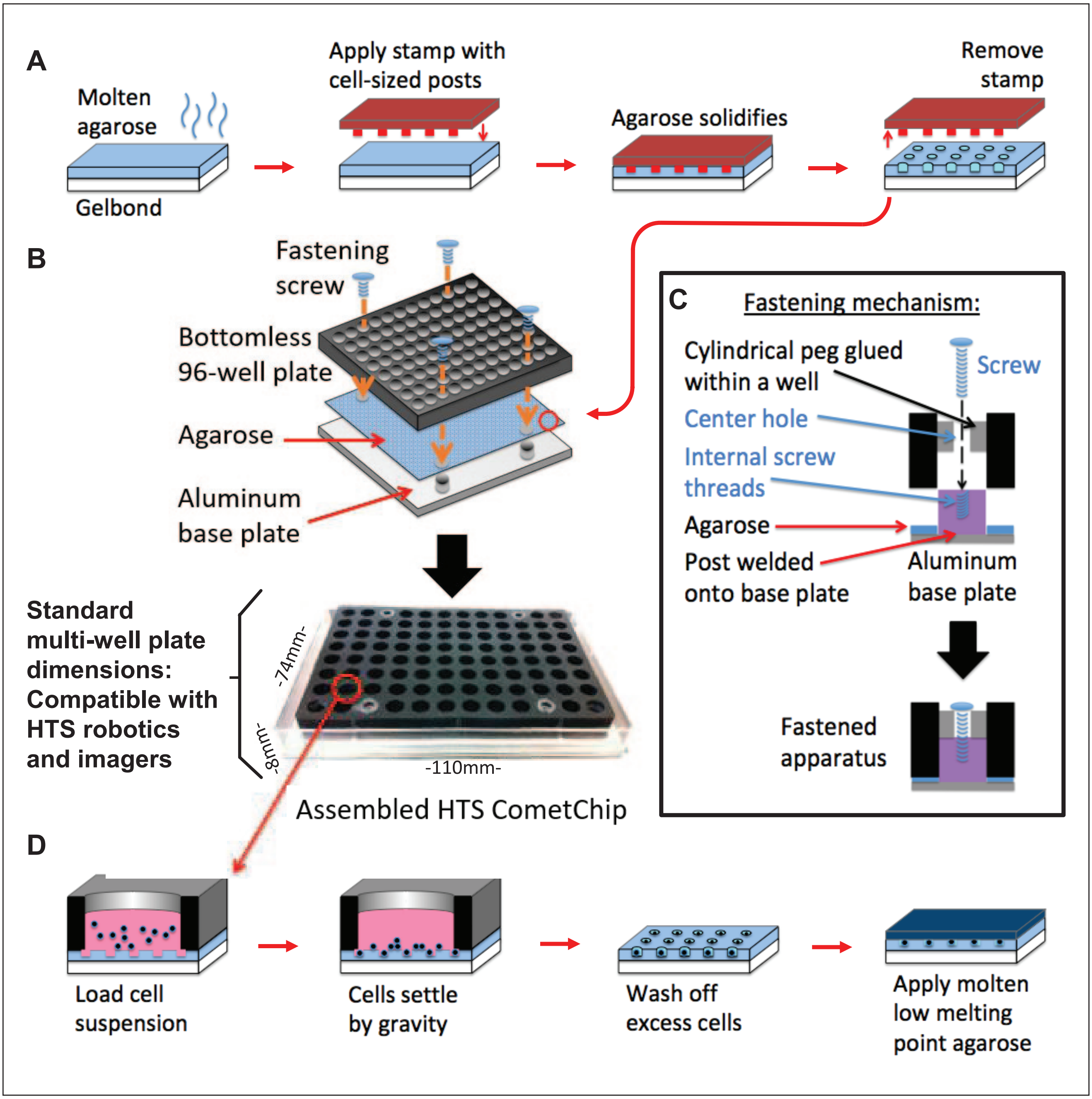

Figure 1. Creation of an HTS-compatible CometChip platform. (**A**) Molten agarose is poured onto a GelBond film and patterned with cell-sized microwells using a microfabricated PDMS stamp. (**B**) The patterned agarose is sandwiched between an aluminum base plate and a modified bottomless 96-well plate. (**C**) The bottomless 96-well plate and the aluminum base plate are clamped together using a set of four screw systems. (**D**) After the apparatus is assembled, a single cell suspension is added to each of the 96 wells and cells settle into the microwells by gravity. Excess cells are washed off and low-melting-point agarose is applied to entrap cells that entered the microwells.

Swanson Biotechnology Center, High Throughput Sciences Facility. Robotic manipulation of the HTS CometChip was performed using a Evo 100 liquid handler (Tecan, Inc., Mannedorf, Switzerland), equipped with a 96-well MultiChannel Arm (MCA96) and a Robotic Manipulator Arm. The Evo 100 is also integrated with a Liconic (Woburn, MA) STX110 incubator with temperature, humidity, and CO_2 control. Imaging of the HTS CometChip was performed using a Thermo Scientific Cellomics ArrayScan VTI HCS Reader with a 5× objective.

Pilot shRNA Screen

Lentiviral reagents expressing shRNA were obtained from the Genetic Perturbation Platform of the Broad Institute of MIT and Harvard (https://portals.broadinstitute.org/gpp/public/). The list of shRNA IDs and their target sequences used in the pilot screen are shown in **Supplemental Figure S1**. M059K cells were plated on five tissue culture 96-well plates at a cell density of 600 cells/well, infected with lentiviruses with an average multiplicity of infection (MOI) of 8, 24 h after cell plating, and selected with 1.5 µg/mL puromycin 48 h after infection. Puromycin was applied for 72 h and cells were allowed to recover in selection-free media for 24 h. All media changes were performed using a EL406 microplate washer (BioTek, Winooski, VT) under sterile conditions. Transfer of cells from tissue culture plates to HTS CometChips was performed using HTS robotics equipment (see above). During the transfer, media was first removed from the tissue culture plates before trypsin was added to dislodge the cells. Plates were returned to a 37 °C incubator for 5 min. After trypsinization, media was added to quench the trypsin and triturated to create single cell suspensions in each well. Cell suspensions from each tissue culture plate were transferred onto an HTS CometChip and allowed to incubate at 37 °C for 20 min. Excess unloaded cells were washed off and a thin layer of low-melting-point agarose was applied to encapsulate cells trapped in microwells. The HTS CometChip assigned as nontreated control was lysed immediately, while the four remaining HTS CometChips were submerged in media and treated with 100 Gy of γ-rays at 1 Gy/min using a ^{137}Cs source. Cells were allowed to repair DNA damage at 37 °C for 0, 1, 2, or 4 h in media before they were lysed. The neutral comet assay was then performed as described above to measure the extent of DNA DSBs.

HTS CometChip shRNA Screen

Lentiviral reagents expressing shRNA were obtained from MIT's Koch Institute of Integrative Cancer Research, Swanson Biotechnology Center, High Throughput Sciences Facility. This shRNA library was purchased from the Broad Institute of MIT and Harvard, The RNAi Consortium (TRC) as a subgenome library of 2564 genes, with three unique shRNAs per gene. The genes targeted by this library are included in the supplemental material available online and additional clone information is available at Broad link: https://portals.broadinstitute.org/gpp/public/.

This library was formatted as an arrayed library, with lentivirus targeting one gene in each well of a 96-well plate, across 89 plates. The screening effort was divided into alternating screening days and imaging days. Prior to screening days, M059K cells were plated on duplicate tissue culture 96-well plates at a density of 600 cells/well, with the exception of 3 wells on each plate to allow the inclusion of untransduced M059K cells (2 wells) and untransduced M059J cells (DNAPKcs null; 1 well). Cells were infected with lentiviruses at an average MOI of 8 the next day after cell plating. One well was infected with a separate preparation of DNAPKcs shRNA that performed best in the pilot screen. Transduced cells were selected with 1.5 µg/mL puromycin 48 h after infection. Puromycin was applied for 72 h and cells were allowed to recover in selection-free media for 24 h. All media changes were performed using a BioTek EL406 microplate washer under sterile conditions. On screening days, cells were transferred to HTS CometChips as described above. CometChips were then submerged in media and treated with 100 Gy of γ-rays at 1 Gy/min using a ^{137}Cs source. Cells were allowed to repair DNA damage at 37 °C for 4 h in media before they were lysed overnight. On imaging days, the HTS CometChips were washed thrice with neutral electrophoresis buffer and electrophoresis was conducted to measure the extent of DNA DSBs. HTS CometChips were stained with SyBR Gold and imaged with a Thermo Scientific Cellomics ArrayScan VTI HCS Reader using a 5× objective.

Transfection with siRNAs

Negative control siRNA (cat. 4390843) and siRNAs targeting LATS2 (cat. 4392420, ID s25505) and DNAPKcs (cat. 4390824, ID s774) were purchased from Ambion (Thermo Scientific) and dissolved in nuclease-free water. HeLa cells (40,000) were plated on each well of a 6-well plate and transfected with siRNA reagents 24 h later as per the manufacturer's instructions.

qRT-PCR

Total RNA was extracted from approximately 500,000 HeLa cells treated with LATS2 or negative control siRNA using RNeasy kit (Qiagen, Germantown, MD). Complementary DNA was generated using random hexamers with M-MLV reverse transcriptase (Invitrogen) according to the manufacturer's instructions. Semiquantitative PCR was performed using an 7500 Fast Real Time PCR System machine (Applied Biosystems, Thermo-Fisher Scientific, Waltham, MA), with Fast SYBR Green master mix (Applied Biosystems) using the following primers: actin (forward)—AGA GCT ACG AGC TGC CTG AC, actin (reverse)—AGC ACT GTG TTG GCG TAC AG, LATS2 (forward)—TCA GAC AGG ACA GCA TGG AG, and LATS2 (reverse)—TAG TTT GGA GTC CCC ACC AG. Data from the experiment were analyzed using the $\Delta\Delta C_T$ method.

Western Blotting

M059K cells were treated with lentiviral shRNA constructs targeting DNAPKcs or GFP, and whole-cell lysates were harvested after successful transduction. Whole-cell lysates were collected using RIPA buffer (Pierce, Thermo-Fisher Scientific, Waltham, MA) supplemented with HALT protease inhibitor (Thermo-Fisher Scientific) and frozen at −20 °C. Lysates were thawed on ice and spun down at maximum speed for 15 min. Lysates were mixed with Laemmli sample buffer (Bio-Rad, Hercules, CA) according to the manufacturer's instructions and incubated at 95 °C for 5 min and then chilled on ice. Samples were loaded onto a 6% sodium dodecyl sulfate–polyacrylamide gel electrophoresis (SDS-PAGE) gel and electrophoresed at 200 V for about 90 min with Tris-glycine-SDS running buffer (Bio-Rad). Proteins were transferred onto nitrocellulose membranes (Bio-Rad) at 100 V for 2 h in Tris-glycine-methanol transfer buffer (Bio-Rad). Membranes were blocked in Odyssey blocking buffer (LI-COR, Lincoln, NE) for 2 h at room temperature with gentle shaking. DNAPKcs and Ku80 were probed with primary antibodies (Cell Signaling Technologies [Beverly, MA] cat. 4602 and cat. 2180) in blocking buffer overnight at 4 °C with gentle shaking. Secondary antibodies (LI-COR) were applied to the membrane in blocking buffer for 2 h at room temperature with gentle shaking. HeLa cells treated with LATS2 or negative control siRNA were treated with 10 Gy of ionizing radiation and allowed to incubate at 37 °C, 5% CO_2 for up to 1–24 h. Whole-cell lysates were collected using whole-cell lysis buffer (0.12 M Tris-HCl, pH 6.8, 4% SDS). Lysates were sonicated at 35 amplitude for 1 min in a cup-horn sonicator. Lysates were mixed with Laemmli sample buffer and incubated at 95 °C for 5 min and separated by SDS-PAGE gels (15% for H2AX, 6% for LATS2). Proteins were transferred onto nitrocellulose membranes (Bio-Rad) at 30 V for 20 h in Tris-glycine transfer buffer. Membranes were blocked in Odyssey blocking buffer (LI-COR) for 2 h at room temperature with gentle shaking. Total H2AX and γH2AX were probed with primary antibodies (Abcam [Cambridge, MA] cat. Ab11175 and EMD Millipore [Burlington, MA] cat. 05-636) in blocking buffer overnight at 4 °C with gentle shaking. Secondary antibodies (LI-COR) were applied to the membrane in blocking buffer for 2 h at room temperature with gentle shaking. Bands were visualized using a LI-COR Odyssey scanner.

CellTiter-Glo Assay

HeLa cells treated with LATS2 or negative control siRNA were treated with up to 20 Gy of ionizing radiation in 96-well plates and allowed to recover for 3 days before performing the CellTiter-Glo assay. Fifty microliters of reconstituted CellTiter-Glo reagent (Promega, Madison, WI) was added to each well containing 50 µL of media and allowed to incubate in room temperature for 10 min with gentle shaking. Analyte was transferred to a white 96-well plate (Evergreen Scientific, Buffalo, NY) and analyzed with a Tecan M1000 plate reader, with an integration time of 1 s per well.

Annexin V Staining

HeLa cells treated with LATS2 or negative control siRNA were transferred onto HTS CometChip and analyzed immediately or after 4 h of incubation at 37 °C in media by annexin V staining (Life Technologies, Thermo-Fisher Scientific, Waltham, MA) according to the manufacturer's instructions. DNA was stained using Vybrant DyeCycle Violet stain (Life Technologies).

Results

Fabrication of HTS CometChip Apparatus

The CometChip was developed to improve the precision and throughput of DNA damage measurements.[26–28] Patterned microwells dictate the positions of cells within an array, which minimizes the footprint per sample, avoids overlapping comets, and facilitates automated imaging and image analysis (**Fig. 1A**). In the initial development of the CometChip, multiple sample areas were created by clamping together a bottomless 96-well plate against a slab of agarose harboring thousands of microwells. When assembled, each well of the 96-well assay plate contains ~300 microwells, which when loaded and processed gives rise to hundreds of comets per sample. Although the CometChip successfully enables processing of multiple samples in parallel, the irregular dimensions of the original CometChip apparatus and of the commercially available apparatus render these platforms incompatible with HTS robotics. To make it possible to leverage the CometChip for HTS experiments using HTS technology, here we describe a novel apparatus designed to be compatible with robotic equipment. Such compatibility greatly expands the versatility of the CometChip, by allowing automation of repetitive pipetting cycles and thereby enabling large-scale screening of existing genetic and chemical libraries that would otherwise be impractical. In order for the assay to achieve compatibility with HTS robotics, two conditions must be fulfilled: (1) robotic manipulator arms must be able to securely lift up and move the assay plate, and (2) a 96-well robotic multichannel pipetting device must be able to accurately dispense reagents into wells. To adapt the HTS CometChip to the HTS robotic environment, we worked with the most common type of robotic manipulator arm, which consists of two parallel grippers. These grippers converge to pick up assay plates. The interaction between assay plates and the robotic manipulator arm requires the assay plate's exterior profile to match that of a typical 96-well plate. Our strategy was therefore to design the apparatus such that it is fully confined within the boundaries of a commercially available uniwell tray that has the dimensions of a 96-well plate (**Fig. 1B**). By using the uniwell tray to create outer dimensions of a typical multiwell plate, we ensured that robotic arms and manipulators can pick up the HTS CometChip, fulfilling the first condition for HTS compatibility. To meet the second requirement (e.g., liquid handling robotics need to correctly dispense contents into each of the 96 wells), we designed the apparatus such that the positions of 96 wells within the apparatus would be consistent across assay plates. To accomplish this, we created a base plate that ensures consistent positioning of the wells. Specifically, the apparatus consists of a lightweight and rigid aluminum base plate with welded posts at positions corresponding to wells A3, A10, H3, and H10 of a standard bottomless 96-well plate (**Fig. 1B**). The aluminum plate was cut to fit snugly within the uniwell tray, thus locking the 96 wells into position. With the goal of clamping a bottomless 96-well plate against a bed of microwells in agarose, a micropatterned agarose slab harboring thousands of microwells is cast onto GelBond film to create the bottom surface. In all of these experiments, the size of the microwells was tuned to be similar to the diameter of a single cell (20–25 μm). The GelBond is punctured to create holes that allow the posts to pass through at positions A3, A10, H3, and H10. The agarose slab is then slotted into position over the aluminum plate.

Next, we clamped a bottomless 96-well plate onto the gel surface, so that each of the 96 wells had hundreds of microwells at its base, as was done previously for the CometChip. In order to attach a commercially available 96-well plate to the aluminum base, we sacrificed 4 wells so that they could be used as attachment points. Specifically, hollow pegs (e.g., polystyrene cylinders), each with a 2 mm hole in their centers, were fused to the inner surface of wells (**Fig. 1C**). The bottomless 96-well plate with its cylindrical pegs is then aligned with the posts on the aluminum base plate. Screws are inserted through the 2 mm holes within the pegs, and they engage the threaded posts (**Fig. 1C**). The screw heads were wider than the holes in the pegs, so tightening the screws provides a clamping force between the bottomless 96-well plate and the base plate, with the agarose in between. The clamping force ensured sealing of wells between the agarose and the bottomless 96-well plate, so that any contents added into the wells would be confined within them. The bottomless 96-well plate was fixed into position by aligning the polystyrene pegs to the aluminum posts on the base plate. Since the aluminum base plate fits snuggly into the uniwell tray, the 96 wells are fixed into position. This ensures that the position of the wells relative to the edges of the assay is identical each time the assay is assembled, fulfilling the second condition for HTS compatibility. Through iterations, we learned that positions A3, A10, H3, and H10 for the pegs optimize even clamping pressure, which prevents leakage from one well to the next.

Once assembled, the HTS CometChip is placed on the work area of HTS robotic equipment. The robot pipettes cell suspensions into each well of the HTS CometChip, transfers the HTS CometChip into a 37 °C incubator for cell loading, and retrieves it after wells have been loaded with cells by gravity (**Fig. 1D**).The HTS CometChip is then disassembled, and the agarose is rinsed to remove excess unloaded cells. A thin layer of low-melting-point agarose is then applied to trap the cells that entered the microwells (**Fig. 1D**). Cells in the agarose can then be exposed to a DNA-damaging agent (e.g., chemicals or ionizing radiation), and cells are allowed to repair the damage by submerging the agarose in growth media. The agarose is then processed for comet analysis using standard procedures, which include (1) incubation in lysis buffer, (2) exposure to an electrophoretic current, and (3) labeling with a DNA stain (see Materials and Methods). Images are then collected and analyzed to quantify the extent of DNA damage (lengths of comet tails) and apoptosis (shapes of comet tails; as described below).

Functional Testing of HTS CometChip

To explore the possibility of using the HTS CometChip for large-scale experiments using HTS robotics, we tested the performance of our apparatus under a range of γIR doses. In order to specifically assess the efficacy of our approach in detecting DNA DSBs, we used the human glioblastoma cell lines M059K and M059J.[29] Derived from the same tumor, the M059J cell line has a truncation mutation in the DNAPKcs gene,[30] whereas the M059K cell line has intact wild-type (WT) DNAPKcs. Given the importance of the core components of the NHEK pathway for DSB repair, we reasoned that these two cell lines should give significant differences in DSB persistence following γIR exposure. Previous studies from our group using neutral CometChip also demonstrate elongated comet tails indicative of decreased DNA DSB repair capacity in cells treated with DNAPKcs chemical inhibitors prior to exposure to DNA DSB-inducing agents.[27] We therefore treated M059K and M059J cells on the HTS CometChip with increasing doses of γIR and allowed them to repair the resulting DNA damage over time. We performed the neutral HTS CometChip assay, as the neutral CometChip had previously been shown to be effective for the detection of DSBs.[27,31] We observed that irradiation led to a dose-dependent increase in the comet tail lengths (**Fig. 2A**). In addition, we also observed a marked difference in the lengths of the comet tails, with the M059J cells showing longer tails (consistent with previous studies[32]). Over time, as DSBs are repaired, the lengths of the comet tails were reduced. Qualitative data showed that there was a significant delay in DSB repair for the repair-deficient M059J cells, as expected (**Fig. 2B**). To gain quantitative results, we analyzed comets from 90 wells across three 96-well HTS CometChips, with each HTS CometChip being exposed to different doses of γIR (**Fig. 2C**). We observed that M059J cells consistently showed

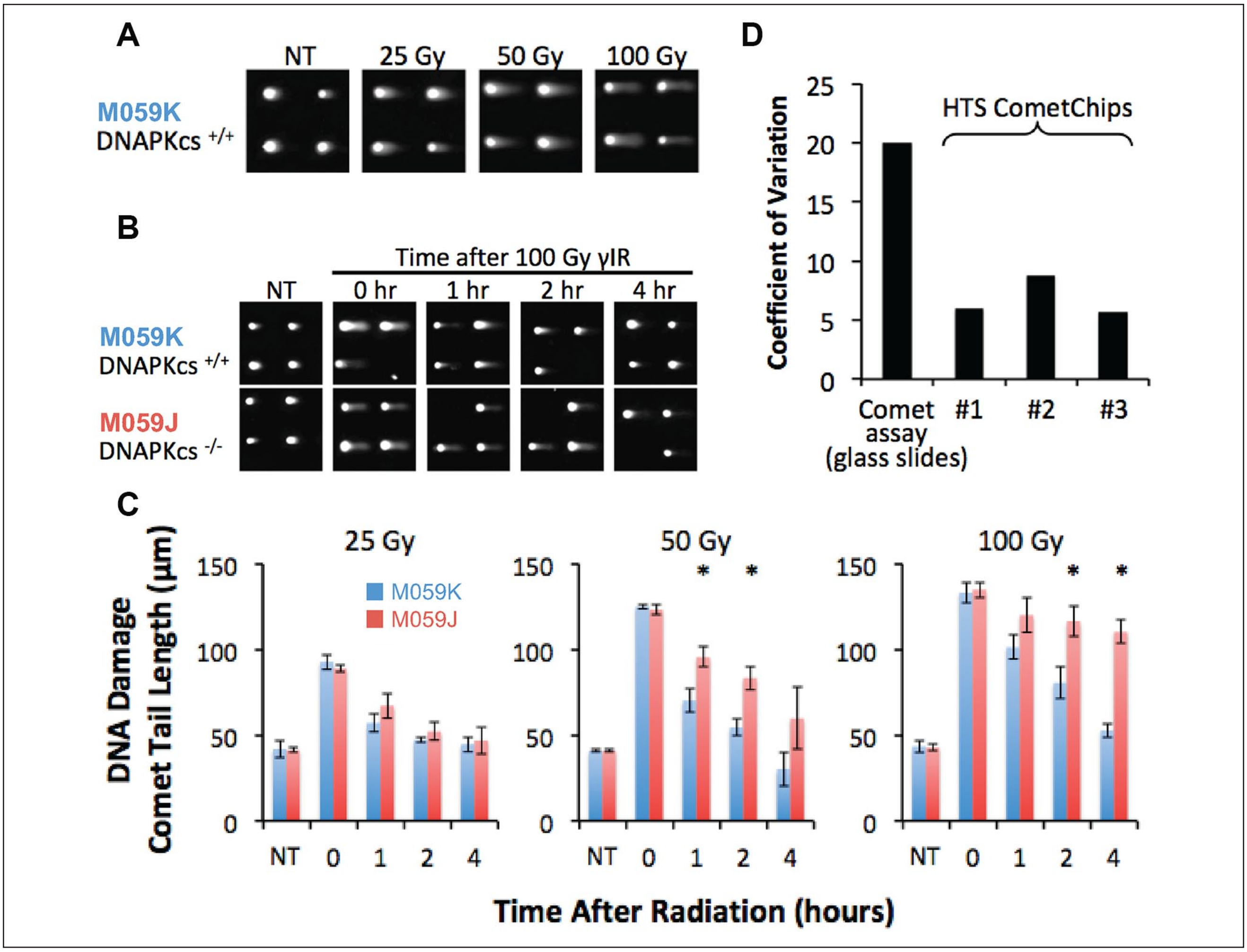

Figure 2. HTS CometChip assay characterization. (**A**) M059K and M059J cells were loaded into 3 HTS CometChips, treated with 25, 50, or 100 GyγIR, and allowed to repair the damage for 1, 2, or 4 h. Representative images immediately after each radiation dose are shown. (**B**) Representative images from the HTS CometChip, which was exposed to 100 GyγIR and allowed to repair for up to 4 h. (**C**) Comet tail lengths from the images were quantified and plotted. Bars show the average of three wells and error bars represent 1 SD. (**D**) COV between wells from three HTS CometChips loaded with M059K cells and treated with 50 GyγIR.

higher levels of DNA damage 1–4 h after exposure to γIR as compared with M059K cells, and increasing doses of γIR led to larger differences in levels of DNA damage between M059K and M059J cells (**Fig. 2C**). Of note, the difference between M059K and M059J was greatest at 4 h after 100 GyγIR exposure (**Fig. 2C**, right panel), conditions that were subsequently adopted for the subsequent shRNA screens. In addition to identifying an optimal time for comet analysis, these experiments also demonstrate that our approach is effective for analysis of many samples across multiple HTS CometChips in parallel. With the goal of analyzing more than 7000 conditions, the HTS CometChip enables a screen that would not be possible with the traditional comet assay (wherein a separate agarose suspension is needed for each sample) or with the original CometChip (wherein the incompatibility of the assay with HTS robotics severely limits its throughput).

Next, we tested the consistency of the data obtained among three HTS CometChips exposed to the same treatment conditions. We found that the coefficient of variation (COV) between wells on each HTS CometChip was between 5% and 10%, consistent with the original version of CometChip[27] and lower than the traditional comet assay (**Fig. 2D**; values in the literature range from ~15% to 20%).[33] We also analyzed the COV of the data in **Figure 2C** by pooling the nontreated condition across three HTS CometChips, and we found that the results for M059K and M059J cells had COVs of 4% and 8%, respectively, which is significantly lower than the traditional assay when performed in our laboratory (~20%). Together, these results

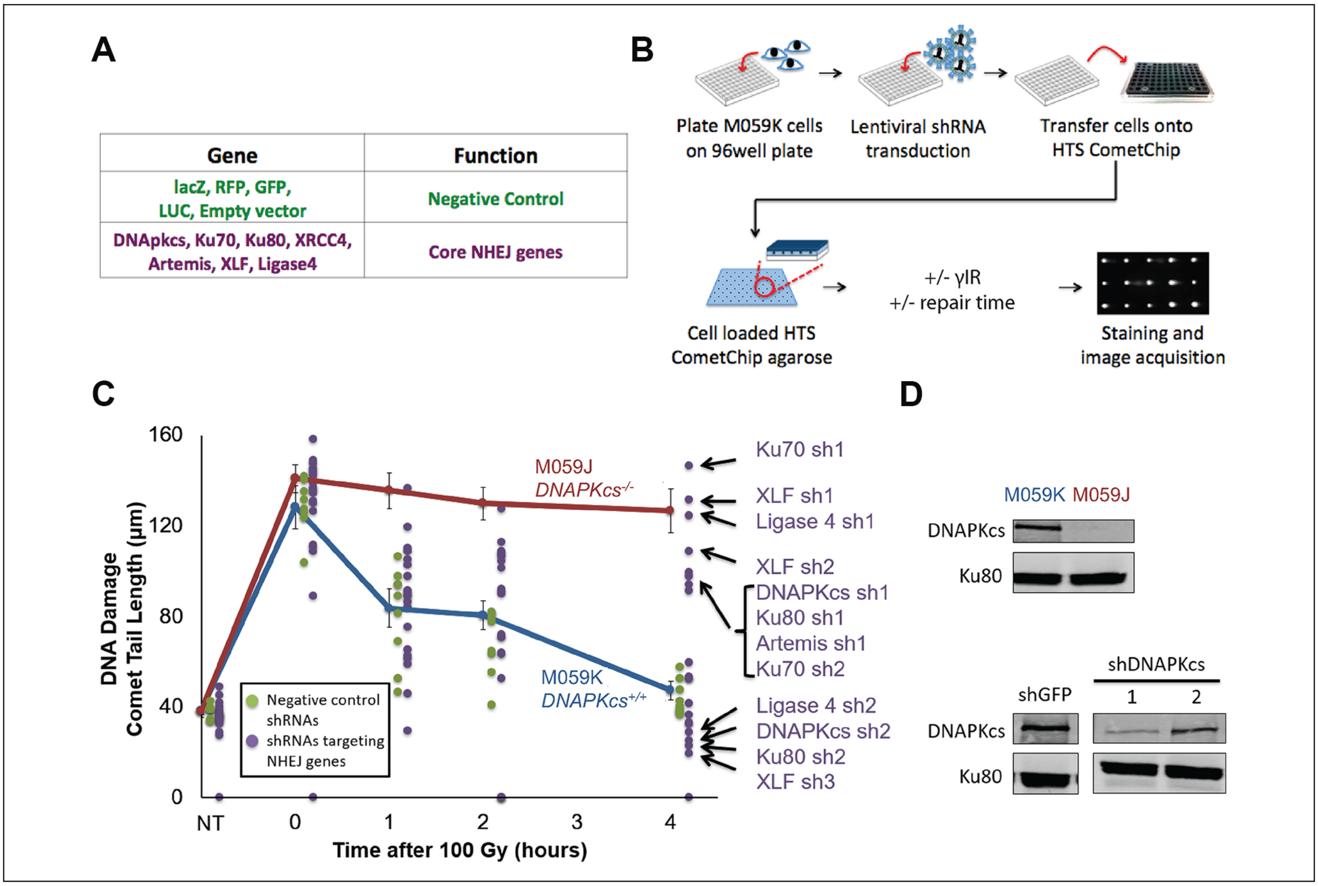

Figure 3. High-throughput shRNA pilot screening using the HTS CometChip. (**A**) Table of genes selected for pilot screening. Genes were color-coded according to their functions. (**B**) A schematic of the steps taken to perform HTS CometChip shRNA pilot screen. M059K cells were plated on tissue culture 96-well plates and transduced with lentiviral shRNAs. Cells were trypsinized and transferred to HTS CometChips. HTS CometChips loaded with cells were treated with 100 Gy γIR and allowed to repair the damage in media. HTS CometChips were placed in lysis buffer overnight, electrophoresed, and stained, and images of the resulting comets were taken. (**C**) Comparison between M059K cells treated with negative control shRNAs and shRNAs targeting NHEJ genes. Each dot represents data from 1 shRNA. (Line graphs represent average comet tail length and error bars represent 1 SD.) (**D**) Western blot confirming more efficient knockdown of DNAPKcs using shDNAPKcs-1 as compared with shDNAPKcs-2. M059K and M059J cells were used as DNAPKcs probing controls. Ku80 was used as a loading control.

showed that with the HTS CometChip, large-scale experiments can be conducted with the aid of automation, and the data produced are more consistent than those of the traditional comet assay.

Pilot Screening

Having demonstrated the efficacy of the HTS CometChip assay for measuring DSBs, we next performed a pilot shRNA screen of key NHEJ genes that should inhibit DSB repair, along with negative controls predicted to have no effect on DSB repair. We designed a custom-made 96-well plate of lentiviruses expressing shRNAs targeting canonical NHEJ genes or negative controls (**Fig. 3A**). Each negative control gene was targeted using two unique shRNAs, and each NHEJ gene was targeted using three unique shRNAs. The top and bottom rows of the plate were used for untransduced M059K and M059J cells, as repair-proficient and -deficient controls, respectively. To test the shRNAs, we first plated M059K cells and added the arrayed lentiviruses (**Fig. 3B**). The transduced cells were transferred onto HTS CometChips by HTS robotics. The untreated control HTS CometChip was submerged into lysis buffer immediately after plating, to allow us to assay for the background levels of DNA DSBs in the cells. All the other HTS CometChips were irradiated. To test for immediate induction of DNA damage, one plate was lysed directly after irradiation to capture the maximum DSB levels. The remaining plates were incubated at 37 °C in complete media to allow time for cells to repair DNA DSBs. For this small screen, plates were incubated for up to 4 h prior to cell lysis and then processed for comet analysis.

In our pilot screen, we assessed the performance of the HTS CometChip under screening conditions. Similar to our earlier assay performance tests, we observed that under lentiviral shRNA screening conditions, untransduced cells proficient in DSB repair (M059K) show robust DNA repair, while M059J cells show reduced repair (blue and red lines, respectively; **Fig. 3C**). At 4 h after γIR, comet tail lengths form lentiviral transduced cells (purple dots; **Fig. 3C**) clustered roughly into two groups: one showing relatively normal levels of DNA repair and the other showing more persistent DNA damage. Cells transduced with negative control shRNAs behaved similarly to the M059K untransduced cells (green dots; **Fig. 3C**), while cells transduced with shRNAs targeting six out of seven NHEJ genes were in the cluster of cells showing reduced repair (**Fig. 3C**).

In some cases, we observed differing results from shRNAs targeting the same gene. We anticipated that this could be the case, given that some shRNAs can be less effective than others. We further explored this possibility by studying the knockdown efficiency for two of the shRNAs targeting DNAPKcs by Western blot. As shown in **Figure 3D**, we found that shRNA 1 had highly efficient knockdown (corresponding with high levels of persistent DNA DSBs; **Fig. 3C**), while shRNA 2 had poor knockdown (**Fig. 3D**), and demonstrated intact repair (**Fig. 3C**), showing the ability of the assay to detect on-target effects. With regard to analysis at different time points, we found that for positive and negative controls, the maximum difference in comet tail length was again observed at 4 h following radiation exposure, and so we selected the 4 h time point for our large-scale screen.

Large-Scale Arrayed Lentiviral shRNA Screen for Modulators of DNA DSB Repair

We next leveraged the HTS CometChip assay to perform a large-scale arrayed shRNA library screen. The shRNA library was created by the Broad Institute as a curated subset of TRC genomic shRNA library. We specifically selected a library that harbors shRNA for oncology-related targets. This library is composed of 7692shRNAs, targeting 2564 key cancer pathway genes. This library was focused on cancer cell signaling, and therefore excluded many essential genes (such as core DNA replication machinery), whose loss would lead to cell death. The arrayed library was prepared in 89 tissue culture 96-well plates (**Fig. 4A**). Each gene was targeted with three unique lentiviral shRNA constructs (predicted to be effective), and each well in every library plate contains one unique shRNA lentivirus. As many NHEJ-directed shRNAs were also not represented in this library, and to allow plate-to-plate comparisons, in each screening plate we included the best-performing lentivirus shRNA against DNAPKcs, and the repair-deficient cell line (M059J) as positive controls and the untransduced repair-proficient cell line (M059K) as well as several nontargeting shRNAs as negative controls.

In order to efficiently assay a large number of plates in the screen, we designed a workflow that uses a staggered format (**Fig. 4B**). To help to ensure that quality data are included for analysis, we rejected any sample with fewer than 20 comets. For each plate, comet lengths for each well (corresponding to cells transduced with a single shRNA) were normalized using the values obtained for M059J and M059K on the same plate. We then took the average value for each of three technical replicates within each plate. Gene scores were calculated using the data from the top two shRNAs for each gene (we omitted data from the least impactful shRNA, since a negative result could be due to inefficient targeting). The normalized data set was then rank-ordered, as shown in **Figure 4C**. The overall average comet tail lengths obtained for the M059K and M059J controls were 58 ± 13 and 120 ± 11 μm, respectively. After normalization, the averages of the negative control shRNAs (against luciferase and lacZ) were 67 ± 12 and 66 ± 11 μm, respectively. On the other hand, the average of the DNAPKcs positive control shRNA was 85 ± 13 μm and was significantly higher than that of all the negative controls (adjusted p values = 2.6×10^{-10}, Tukey's multiple comparisons test). The repair-deficient M059J cells are far to the left on the rank-ordered graph, whereas the repair-proficient M059K cells are far to the right, supporting the efficacy of the approach. It is noteworthy that the DNAPKcs shRNA shows a partial phenotype, discussed below.

Screen of 2564 Genes Reveals LATS2 as a Top Hit for DNA Fragmentation

We interrogated which pathways were represented in the top 150 genes from our screen by performing Ingenuity Pathway Analysis (**Fig. 5A**). In general, we expect pathways that modulate DNA DSB repair in cells to score highly in our screen. However, as the library was designed for therapeutic target discovery in cancer, many essential and core DNA repair factors were not represented. Therefore, as expected, canonical genes that code for components directly involved in NHEJ were not identified among our hits. However, pathways with known roles in DNA damage were clearly identified. In fact, we found that the top pathway identified was 14-3-3 signaling. Specifically, two out of the seven core 14-3-3 genes (YWHAQ, also known as 14-3-3 tau; SFN, also known as 14-3-3 sigma) were represented in our top 150 gene list. It has previously been shown that 14-3-3 proteins bind and modulate many DNA repair factors, in turn affecting cellular resistance to several cancer therapies, including radiotherapy.[34,35] The observation that 14-3-3 shows up as the top pathway therefore both solidifies our understanding of the role of 14-3-3 in DNA repair

A

Total number of genes targeted	2564
Total number of shRNAs	7692
Genes in library also present in pilot screen	DNAPKcs, NHEJ1
Each plate contains:	
Repair proficient controls	M059K (WT), shGFP, shLuciferase, shLacZ
Repair deficient controls	M059J (WT), shDNAPKcs-1* (independently prepared)
Lentiviruses targeting 29 genes	1 well per shRNA, 3 shRNAs per gene

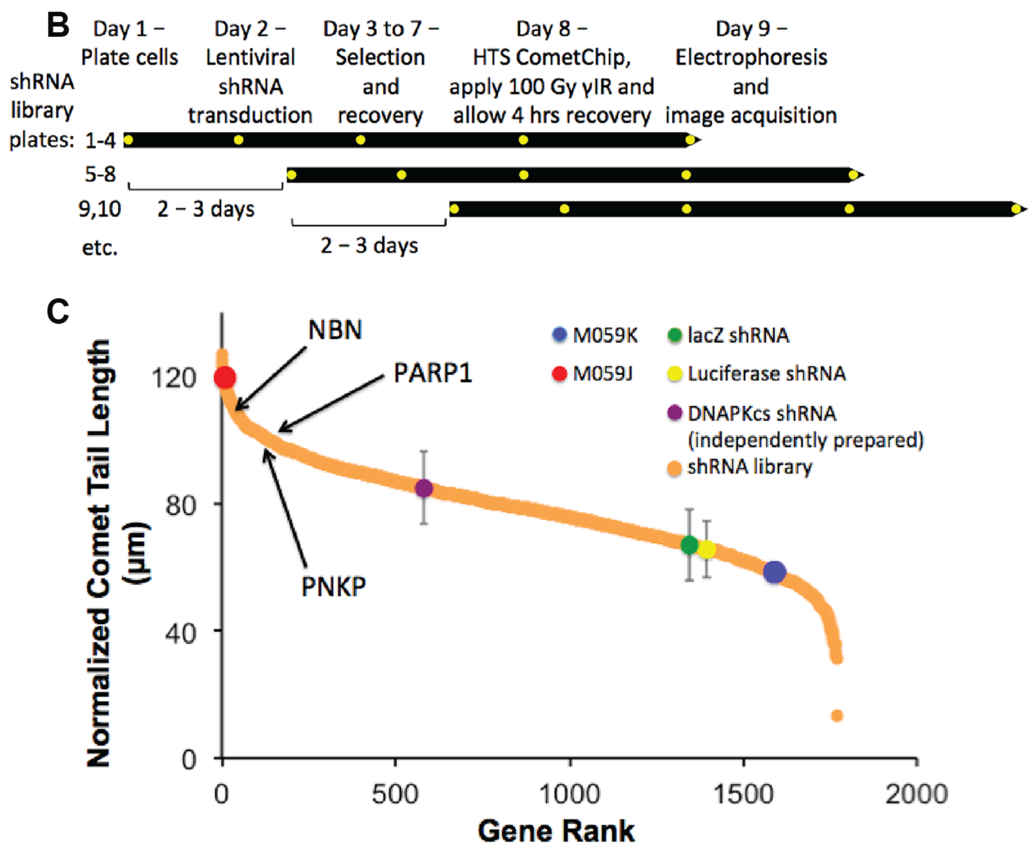

Figure 4. Large-scale arrayed lentiviral shRNA screen for modulators of DNA DSB repair. (**A**) Contents of the large-scale lentiviral shRNA library. (**B**) A schematic of how the screen was performed. The screen was conducted in batches of two or four library plates, with a 2- to 3-day delay between batches. Each library plate was applied to M059K cells and the cells were selected for successful transduction before transferring them to HTS CometChips. Cells in HTS CometChips were treated with 100 Gy γIR and allowed to repair the damage in media for 4 h before overnight lysis. HTS CometChips were then electrophoresed and imaged. (**C**) Genes from the screen, rank-ordered according to the averaged normalized comet tail lengths of the top two shRNAs for each gene. shRNAs represented by fewer than 20 comets on either replicate were removed from analysis.

and provides additional evidence that our screen is effective for identifying genes and pathways that modulate DNA repair activity in cells.

The second most significantly enriched pathway identified by Ingenuity Pathway Analysis is the Hippo signaling pathway. The Hippo signaling pathway is known to control the rates of cell growth and organ sizes in an organism.[36] In flies, inactivation of the Hippo signaling pathway leads to tumor-like growth in specific tissues, due to loss of cell–cell contact growth inhibition and overproliferation of the constituent cells.[37] Conversely, deregulation of the Hippo signaling pathway can lead to changes in the cell's response to

A

Canonical pathways	p value	Associated genes
14-3-3 mediated signaling	7.22×10^{-8}	MAP3K5 (5), PIK3C3 (55), PIK3R5 (45), SFN (6), SRPK2 (85), TSC2 (88), VIM (60), YWHAQ (96)
Hippo signaling	1.43×10^{-7}	AJUBA (102), **LATS2 (62)**, PPP1R3A (66), PPP2R2C (77), PPP2R5E (99), SFN (6), YWHAQ (96)
ERK/MAPK signaling	2.28×10^{-7}	PIK3C3 (55), PIK3R5 (45), PPP1R3A (66), PPP2R2C (77), PPP2R5E (99), PRKAR1B (44), PTK2B (15), YWHAQ (96)
IGF-1 signaling	3.48×10^{-7}	PIK3C3 (55), PIK3R5 (45), PRKACG (22), PRKAR1B (44), SFN (6), SOCS1 (23), YWHAQ (96)
p70S6K signaling	1.69×10^{-6}	LYN (36), PIK3C3 (55), PIK3R5 (45), PPP2R2C (77), PPP2R5E (99), SFN (6), YWHAQ (96)

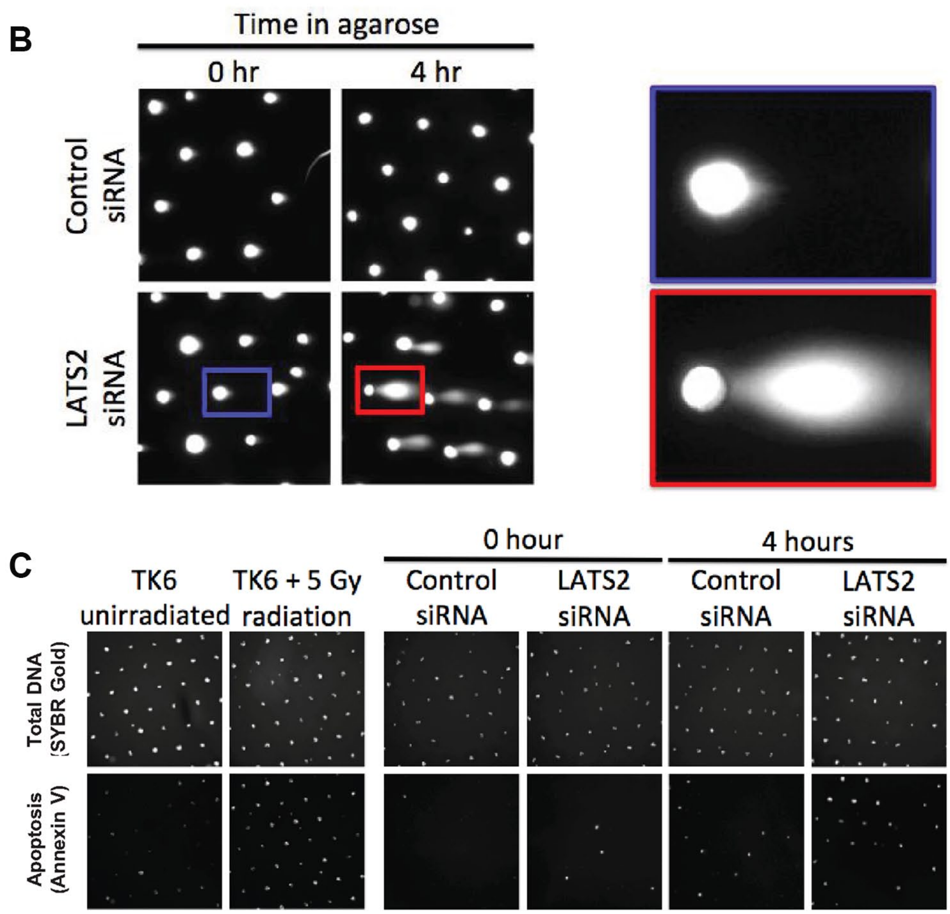

Figure 5. Identification of an apoptotic phenotype in LATS2-depleted cells. (**A**) Highly significant pathways represented within the top 150 genes obtained from Figure 4C, as analyzed by Ingenuity Pathway Analysis software. LATS2 is highlighted in red. (**B**) HeLa cells treated with LATS2 or control siRNA were encapsulated in agarose and allowed to recover in media for 0 or 4 h before lysis. Right inserts show 4× magnification of color-coded box-bounded comets. (**C**) HeLa cells treated with LATS2 or control siRNA were stained with a DNA stain and annexin V immediately or 4 h after they were transferred to HTS CometChip agarose without exposure to DNA damage. TK6 cells treated with 0 or 5 Gy of γIR and incubated for 24 h were used as negative and positive controls for annexin V staining.

pro-apoptotic signals activated by chemotherapeutic agents or changes in anchorage status. Given these known roles of the Hippo signaling pathway, we reasoned that increased DNA fragmentation (longer tails) observed in cells knocked down for Hippo pathway genes could also be due to apoptosis.

To explore the possibility of apoptosis-induced comets in our screen, we analyzed the comet images from RFC5, a gene that is essential for DNA replication, as well as a prominent candidate gene belonging to the Hippo signaling pathway, LATS2. We reasoned that depleting a gene that requires DNA replication will lead to replication fork collapse during the S phase of the cell cycle, and subsequently lead to DSB formation and apoptosis. Indeed, analysis of images from RFC5 in the screen showed that many of the comets have a shape that is characteristic of apoptosis, wherein there is extensive DNA fragmentation[19,20,38–40] (**Suppl. Fig. S2**). We observed similar comet shapes for LATS2 from our screen and hypothesized that LATS2 KD cells might produce apoptotic comets even without γIR exposure. We tested this hypothesis by loading LATS2 KD and control cells onto the HTS CometChip and analyzing them 4 h after incubation at 37 °C in media. We observed that both control and LATS2 KD cells did not show signs of DNA fragmentation when they were first loaded into the HTS CometChip (**Fig. 5B**). However, after allowing the cells to incubate in media in the agarose microwells for 4 h, LATS2 KD cells showed a high percentage of apoptotic comets. Therefore, our screen is effective not only for identifying genes that impact DNA repair, but also for identifying genes that modulate susceptibility to apoptosis under anchorage-independent growth conditions.

To further explore the possibility that LATS2 KD cells are sensitized to apoptosis under anchorage-independent growth conditions, we used an alternative approach for assaying for apoptosis, namely, annexin V staining (**Fig. 5C**). We found that most cells were negative for annexin V staining when they were first placed in the HTS CometChip. Consistent with the appearance of apoptotic tails, when the cells were left in HTS CometChip for 4 h, we observed that ~40% of the LATS2 KD cells were positive for annexin V, compared with low levels of staining for control cells (**Fig. 5C**). Together, these results suggest that downregulation of LATS2 leads to apoptosis upon loss of cell–cell contact, which is consistent with previous studies.[41,42]

LATS2 Knockdown Cells Are Defective in DNA DSB Repair

Several proteins in the Hippo signaling pathway have also previously been shown to be activated when cells are exposed to DNA damage.[43] This led us to hypothesize that LATS2 KD cells might also be deficient in DNA DSB repair. To investigate whether or not LATS2 KD has a DNA repair defect, we treated control and LATS2 KD-irradiated cells and assayed for DNA DSBs. Specifically, we treated HeLa cells with siRNA targeting sequences in LATS2 distinct from the shRNA sequences used in the screening library, and allowed them to recover under adherent conditions on tissue culture plates, thereby maintaining cell–cell contacts, before transferring them to the CometChip to enable studies of DNA damage and repair (rather than apoptosis). In images obtained from these experiments, tail morphology was consistent with DNA damage, rather than apoptosis (**Fig. 6A,B**). Quantitative analysis showed that LATS2 KD cells had longer comet tails indicative of higher levels of DNA damage at all time points assayed after exposure to γIR (**Fig. 6C**). For reference, mRNA and protein levels from control and LATS2 siRNA-treated HeLa cells are shown in **Supplemental Figures S3 and S4**, respectively. Therefore, we conclude that LATS2 downregulation leads to slower DNA DSB repair after cells are exposed to γIR.

As an independent approach for evaluating the levels of DSBs, we also tested the effect of LATS2 KD on the formation of γH2AX after exposure to γIR via Western blotting. We found that LATS2 KD cells have a higher level of γH2AX after being exposed to γIR as compared with control cells, which is consistent with the presence of higher levels of DNA DSBs (**Fig. 6D**). Given that LATS2 KD resulted in a DNA DSB repair defect in cells, we next asked if LATS2 KD cells are more sensitive to cytotoxicity induced by γIR exposure. We found that LATS2 KD cells indeed proliferated at a slower rate when exposed to γIR as compared with control cells (**Fig. 6E**). These results support the hypothesis that LATS2 KD results in diminished DNA DSB repair after exposure to γIR, which correlates with reduced growth rates post-IR exposure as compared with nontreated controls. Taken together, analysis of LATS2 KD cells shows that in addition to its role in promoting cell–cell contact pro-survival signaling, LATS2 also contributes to DNA repair and its deficiency leads to radiation sensitivity.

Discussion

In this study, we developed technology to perform large-scale comet assay-based experiments utilizing HTS robotics and performed a first-of-its kind DNA DSB genetic screen. The original comet assay, although well accepted by the DNA repair community, is an assay that is rarely adopted when researchers intend to perform large-scale experiments. There are two main reasons for this: (1) incompatibility with HTS robotics and (2) the high variability in data produced by the assay. In terms of sample handling, the CometChip alleviates the problems of the comet assay by maximizing the number of comets obtainable per unit area of the assay, which makes it possible to analyze 96 samples on the same assay plate. This reduces the amount of

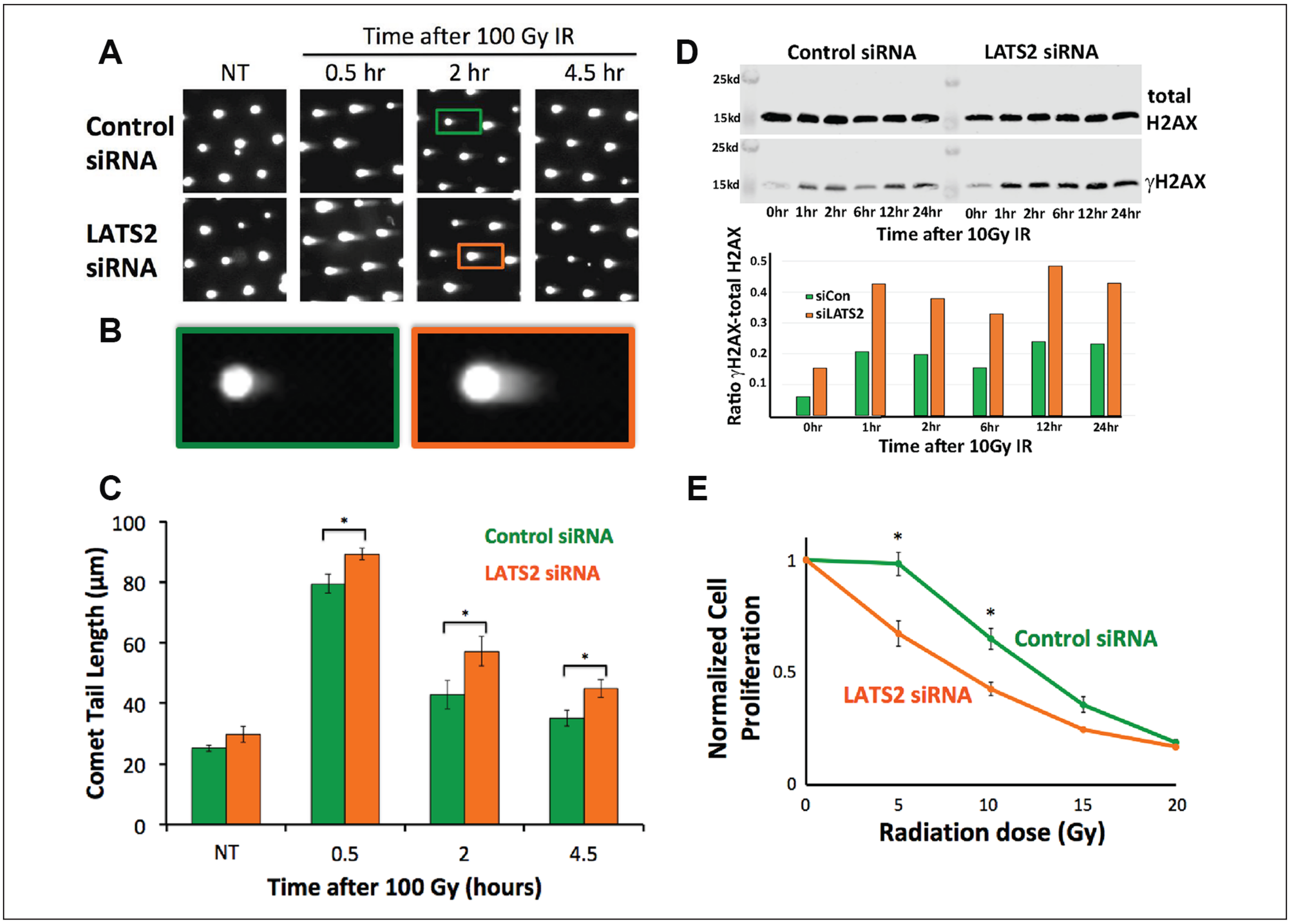

Figure 6. LATS2 knockdown causes DNA DSB repair defects. (**A**) HeLa cells treated with control siRNA (top row) and LATS2 siRNA (bottom row) were treated with 100 Gy γIR and incubated in media before the cells were trypsinized and loaded onto the HTS CometChip. Representative images are shown. (**B**) Comet tail lengths from **A** were quantified ($n = 3$; data points represent mean ± 1 SD; *$p < 0.05$ for paired Student t test). (**C**) Magnification (5×) of color-coded box-bounded comets in **A**. (**D**) Representative Western blots of lysates from HeLa cells transfected with control or LATS2 siRNA that were probed for γH2AX and total H2AX levels at indicated time points following exposure to 10 GyγIR. Bar graphs shows the ratio of γH2AX to total H2AX signals from Western blot. (**E**) Relative cell proliferation of HeLa cells transfected with control or LATS2 siRNA measured by CellTiter-Glo, 72 h after γIR treatment ($n = 3$; data points represent mean ± 1 SD; *$p < 0.05$ for paired Student t test).

preparatory work per sample, therefore making the assay less cumbersome to perform. In terms of reproducibility, testing multiple samples on the same assay plate also reduces noise between samples, therefore reducing variability in the data produced. Furthermore, the regular array of comets produced by the patterned microwells prevents overlapping comets, enabling automated image analysis, which greatly increases the throughput and precision of the assay. While the CometChip is now well established, the HTS CometChip takes the platform a step further, enabling the use of HTS robotics. By leveraging the innovations of robotic screening and further improving precision, speed, and reproducibility, it is now possible to perform large-scale comet assay experiments.

With this platform, we queried a library of 7692 shRNAs targeting 2564 genes to identify gene targets affecting DNA repair following γIR exposure. In addition, since the comet assay detects DNA fragmentation, it was also possible to detect DNA damage from apoptosis. This comprises the first high-throughput genetic screen using physical DNA fragmentation as a readout for apoptosis. Despite the lack of shRNAs targeting canonical DNA repair genes in the screening library, we identified the 14-3-3 signaling as the top pathway from our screen. The 14-3-3 signaling pathway is intimately involved in a cell's DNA damage response, providing evidence that our screening methodology could potentially reveal novel DNA repair genes and pathways. This screen identified LATS2 as an IR-induced DNA damage repair factor. Interestingly, LATS2 also scored in our assay for apoptotic DNA damage. As such, the platform can be used both for studies of apoptosis and for studies of DNA damage and repair.

In our study, we identified the Hippo pathway protein kinase LATS2 as a novel DNA DSB repair modulator. The Hippo pathway was also identified as the second most significantly enriched pathway in the top 150 genes from our screen (7 out of 150 genes). The Hippo pathway is known to control cell growth rates and organs.[36,37,44] The members of the Hippo pathway were first identified in *Drosophila*, where mutant Hippo pathway genes led to massive overgrowth in the organs that harbored the mutated cells. The Hippo pathway consists of four kinases, MST1, MST2, LATS1, and LATS2, which receive input signals from environmental cues such as cell adhesion and cell–cell contact.[45] The end result of the kinase cascade activation in this pathway is the phosphorylation of the YAP/TAZ transcriptional co-activators, leading to their degradation. When the kinases are inactive, YAP and TAZ can translocate into the cell nucleus and promote the activity of TEADs and SMADs, which in turn promotes cell growth and tumorigenesis.[46] In the context of these cell–environment signaling pathways, LATS2 and the Hippo pathway were connected to DNA damage via Abl kinase.[47]

Our data demonstrate that the loss of LATS2 in cells led to sustained levels of DNA DSBs after exposure to γIR, as well as to increased levels of γH2AX signaling. We also observed a radiation-induced growth defect in LATS2-depleted cells. This, coupled with the DSB repair defect we observed, suggests that increased radiation sensitivity could be due to unrepaired DSBs following LATS2 loss of function.

We also observed that LATS2 depletion led to increased comet tail length when the cells were dispersed and transferred from tissue culture plates to agarose. This phenotype was observed even when cells were not exposed to γIR, suggesting that these comet tails could be caused by DNA fragmentation from apoptotic signaling. Since the Hippo pathway responds to changes in cell–cell contacts and to changes in the extracellular matrix environment, we hypothesize that transferring the cells from a monolayer on a tissue culture plate to a low-adherence single-cell 3D environment encapsulated by agarose may change the activity of the pathway, and that loss of LATS2 in this context may lead to activation of apoptosis. We confirmed this by demonstrating annexin V staining in LATS2-depleted cells treated with the same nonirradiated conditions. Therefore, our identification of LATS2 demonstrates the ability of the HTS CometChip to detect modifiers of both radiation- and apoptosis-induced DSBs.

In terms of efficacy for use in a large screen, it is helpful to compare HTS CometChip throughput to what is feasible with the traditional assay. Our screening library was distributed across eighty-nine 96-well plates, with each shRNA occupying a single well. We collected 9 images from each well, capturing an average of 50 comets per shRNA. Including the wells that were assigned for controls on each plate, we collected ~130,000 images, containing more than 750,000 comets. To put the scale of the screen in perspective, given a liberal estimate of being able to complete 100 traditional comet assay slides per week, it would take a typical researcher at least 150 weeks to collect the same amount of data as we did in about 10 weeks. Thus, the HTS CometChip can be used to screen thousands of genes for their potential impact on DNA fragmentation.

Although beyond the scope of this particular study, it is possible to further increase the rate of data collection when using the HTS CometChip in a genomic screen. In our proof-of-concept screen, we fabricated and loaded 8 HTS CometChips at a time each day, taking about 1.5 h to complete. This can be easily quadrupled, to yield data from approximately 2600 samples (32 HTS CometChips × 84 sample wells) per day or 13,000 samples per 5-day workweek. A screen using a typical genomic shRNA library that targets approximately 20,000 genes using three distinct shRNAs per gene will take as little as 10 weeks to complete, with duplicate data for each shRNA. The possibility of performing a genome-wide screen for factors that modulate DNA DSBs by measuring physical DNA damage can now be fully realized with the advent of HTS CometChip as an enabling innovation.

Our study focused on the application of HTS CometChip to detect physical DNA DSBs, but the HTS CometChip can also be used to detect other forms of DNA damage. To discover genes that are involved in DNA DSB repair, we performed the neutral comet assay; however, different conditions can detect other classes of DNA damage. For example, base damage induced by oxidizing or alkylating agents can be detected when it is converted to strand breaks either enzymatically (e.g., during base excision repair) or by incubation under alkaline conditions.[48] Alternatively, it is also possible to detect subclasses of damage such as oxidized purines. These lesions can be detected by incubation with specific endonucleases after cell lysis, which converts undetectable base lesions into detectable abasic sites and/or single-strand breaks.[49] The ability to measure single-strand breaks that are formed during excision repair further expands the utility of the assay by enabling analysis of the DNA repair capacity for damaged bases. Furthermore, the HTS CometChip can also measure epigenetic marks such as DNA methylation. Specifically, the recently reported EpiComet-Chip[50] exploits recognition of 5MeC by the McrBC restriction enzyme, and converts sites of CpG methylation into detectable single-strand breaks. These can then be detected readily by the HTS CometChip. Therefore, we propose that the HTS CometChip is useful for a broad range of applications. Finally, it was recently shown that the microwell platform used for these studies can also be cross-purposed to monitor cell growth, thus facilitating parallel analysis of genotoxicity and cytotoxicity.[51]

All of the proposed variants of the HTS CometChip experiments (e.g., measuring DSBs, alkali-labile sites, base damage, and 5MeC) can also be adapted for small-molecule screens as part of a drug discovery process. Small-molecule libraries are frequently arranged in an arrayed format (each drug/dose condition in the library occupies one well in a multiwell plate), and this format is highly compatible with the arrayed nature of the HTS CometChip. A small-molecule library can also be used in tandem with a DNA damage inducer (such as γIR) to identify DNA repair chemical inhibitors. These inhibitors can form the basis of drug development to produce adjuvant therapies that can enhance the effectiveness of DNA-damaging cancer treatments, leading to improved outcomes.

In conclusion, we have developed the HTS CometChip to render the powerful CometChip technology compatible with automated robotic systems found in HTS facilities. We used this assay to query thousands of genes for their ability to modulate DNA DSB levels by measuring levels of physical DNA DSBs in cells exposed to radiation. From a screen of more than 7500 shRNAs, we identified LATS2 as a gene that, when depleted, leads to inefficient DNA DSB repair and radiosensitivity. We also showed that LATS2-depleted cells undergo apoptosis more readily when they were encapsulated in agarose, indicating that the HTS CometChip can also be used for studies of apoptosis. Given the myriad permutations to the comet assay for detecting different classes of damage, excision repair capacity, and even global methylation levels, the HTS CometChip is an effective tool for performing a broad range of high-throughput screens with applications in cancer biology.

Authors Note

Scott R. Floyd is currently affiliated with Department of Radiation Oncology, Duke University School of Medicine, Durham, NC, USA.

Acknowledgments

This work was made possible with the assistance and expertise of the MIT Central Machine Shop for the fabrication of the HTS CometChip apparatus. We thank the Koch Institute's Robert A. Swanson (1969) Biotechnology Center for technical support, specifically, the High Throughput Sciences Facility.

Declaration of Conflicting Interests

The authors declared no potential conflicts of interest with respect to the research, authorship, and/or publication of this article.

Funding

The authors disclosed receipt of the following financial support for the research, authorship, and/or publication of this article: This work was supported by the Joint Center for Radiation Therapy foundation (JCRT), the Koch Institute Clinical Investigator Award, and the Burroughs Wellcome Career Award for Medical Scientists (awarded to S.R.F.). I.J.T. was supported by the Agency for Science Technology and Research (A*STAR) National Science Scholarship (NSS-PhD), with support from P01CA26731 and R44ES024698 (awarded to B.P.E.). This work was also supported by the MIT Centre for Environmental Health Sciences (P30ES002109), and by the Koch Institute Support (core) Grant P30-CA14051 from the National Cancer Institute.

ORCID iD

Scott R. Floyd https://orcid.org/0000-0002-8067-2426

References

1. Hoeijmakers, J. H. DNA Damage, Aging, and Cancer. *N. Engl. J. Med*. **2009**, *361*, 1475–1485.
2. Hanahan, D.; Weinberg, R. A. Hallmarks of Cancer: The Next Generation. *Cell* **2011**, *144*, 646–674.
3. Cucinotta, F. A.; Nikjoo, H.; O'Neill, P.; et al. Kinetics of DSB Rejoining and Formation of Simple Chromosome Exchange Aberrations. *Int. J. Radiat. Biol*. **2000**, *76*, 1463–1474.
4. Sung, P. Introduction to the Thematic Minireview Series: DNA Double-Strand Break Repair and Pathway Choice. *J. Biol. Chem*. **2018**, *293*, 10500–10501.
5. West, S. C. Molecular Views of Recombination Proteins and Their Control. *Nat. Rev. Mol. Cell Biol*. **2003**, *4*, 435–445.
6. Mao, Z.; Bozzella, M.; Seluanov, A.; et al. DNA Repair by Nonhomologous End Joining and Homologous Recombination during Cell Cycle in Human Cells. *Cell Cycle* **2008**, *7*, 2902–2906.
7. Burma, S.; Chen, B. P.; Chen, D. J. Role of Non-Homologous End Joining (NHEJ) in Maintaining Genomic Integrity. *DNA Repair (Amst.)* **2006**, *5*, 1042–1048.
8. Shao, Z.; Davis, A. J.; Fattah, K. R.; et al. Persistently Bound Ku at DNA Ends Attenuates DNA End Resection and Homologous Recombination. *DNA Repair (Amst.)* **2012**, *11*, 310–316.
9. Davis, A. J.; Chen, B. P.; Chen, D. J. DNA-PK: A Dynamic Enzyme in a Versatile DSB Repair Pathway. *DNA Repair (Amst)* **2014**, *17*, 21–29.
10. Goodarzi, A. A.; Yu, Y.; Riballo, E.; et al. DNA-PK Autophosphorylation Facilitates Artemis Endonuclease Activity. *EMBO J*. **2006**, *25*, 3880–3889.
11. Weinfeld, M.; Mani, R. S.; Abdou, I.; et al. Tidying Up Loose Ends: The Role of Polynucleotide Kinase/Phosphatase in DNA Strand Break Repair. *Trends Biochem. Sci*. **2011**, *36*, 262–271.
12. Fan, W.; Wu, X. DNA Polymerase Lambda Can Elongate on DNA Substrates Mimicking Non-Homologous End Joining and Interact with XRCC4-Ligase IV Complex. *Biochem. Biophys. Res. Commun*. **2004**, *323*, 1328–1333.
13. Ahnesorg, P.; Smith, P.; Jackson, S. P. XLF Interacts with the XRCC4-DNA Ligase IV Complex to Promote DNA Nonhomologous End-Joining. *Cell* **2006**, *124*, 301–313.
14. Ochi, T.; Blackford, A. N.; Coates, J.; et al. DNA Repair. PAXX, a Paralog of XRCC4 and XLF, Interacts with Ku to Promote DNA Double-Strand Break Repair. *Science* **2015**, *347*, 185–188.
15. Gupta, R.; Somyajit, K.; Narita, T.; et al. DNA Repair Network Analysis Reveals Shieldin as a Key Regulator of NHEJ and PARP Inhibitor Sensitivity. *Cell* **2018**, *173*, 972–*988*.e23.

16. Hurov, K. E.; Cotta-Ramusino, C.; Elledge, S. J. A Genetic Screen Identifies the Triple T Complex Required for DNA Damage Signaling and ATM and ATR Stability. *Genes Dev*. **2010**, *24*, 1939–1950.
17. Floyd, S. R.; Pacold, M. E.; Huang, Q.; et al. The Bromodomain Protein Brd4 Insulates Chromatin from DNA Damage Signalling. *Nature* **2013**, *498*, 246–250.
18. Olive, P. L.; Banath, J. P. Detection of DNA Double-Strand Breaks through the Cell Cycle after Exposure to X-Rays, Bleomycin, Etoposide and 125IdUrd. *Int. J. Radiat. Biol*. **1993**, *64*, 349–358.
19. Olive, P. L.; Frazer, G.; Banath, J. P. Radiation-Induced Apoptosis Measured in TK6 Human B Lymphoblast Cells Using the Comet Assay. *Radiat. Res*. **1993**, *136*, 130–136.
20. Choucroun, P.; Gillet, D.; Dorange, G.; et al. Comet Assay and Early Apoptosis. *Mutat. Res*. **2001**, *478*, 89–96.
21. Ostling, O.; Johanson, K. J. Microelectrophoretic Study of Radiation-Induced DNA Damages in Individual Mammalian Cells. *Biochem. Biophys. Res. Commun*. **1984**, *123*, 291–298.
22. Singh, N. P.; McCoy, M. T.; Tice, R. R.; et al. A Simple Technique for Quantitation of Low Levels of DNA Damage in Individual Cells. *Exp. Cell Res*. **1988**, *175*, 184–191.
23. Collins, A. R. The Comet Assay for DNA Damage and Repair: Principles, Applications, and Limitations. *Mol. Biotechnol*. **2004**, *26*, 249–261.
24. Sykora, P.; Witt, K. L.; Revanna, P.; et al. Next Generation High Throughput DNA Damage Detection Platform for Genotoxic Compound Screening. *Sci. Rep*. **2018**, *8*, 2771.
25. Shaposhnikov, S.; Azqueta, A.; Henriksson, S.; et al. Twelve-Gel Slide Format Optimised for Comet Assay and Fluorescent In Situ Hybridisation. *Toxicol Lett*. **2010**, *195*, 31–34.
26. Wood, D. K.; Weingeist, D. M.; Bhatia, S. N.; et al. Single Cell Trapping and DNA Damage Analysis Using Microwell Arrays. *Proc. Natl. Acad. Sci. U. S. A*. **2010**, *107*, 10008–10013.
27. Weingeist, D. M.; Ge, J.; Wood, D. K.; et al. Single-Cell Microarray Enables High-Throughput Evaluation of DNA Double-Strand Breaks and DNA Repair Inhibitors. *Cell Cycle* **2013**, *12*, 907–915.
28. Ge, J.; Prasongtanakij, S.; Wood, D. K.; et al. CometChip: A High-Throughput 96-Well Platform for Measuring DNA Damage in Microarrayed Human Cells. *J. Vis. Exp*. **2014**, *92*, e50607.
29. Allalunis-Turner, M. J.; Barron, G. M.; Day, R. S., III; et al. Isolation of Two Cell Lines from a Human Malignant Glioma Specimen Differing in Sensitivity to Radiation and Chemotherapeutic Drugs. *Radiat. Res*. **1993**, *134*, 349–354.
30. Lees-Miller, S. P.; Godbout, R.; Chan, D. W.; et al. Absence of p350 Subunit of DNA-Activated Protein Kinase from a Radiosensitive Human Cell Line. *Science* **1995**, *267*, 1183–1185.
31. Wang, Y.; Xu, C.; Du, L. Q.; et al. Evaluation of the Comet Assay for Assessing the Dose-Response Relationship of DNA Damage Induced by Ionizing Radiation. *Int. J. Mol. Sci*. **2013**, *14*, 22449–22461.
32. Iliakis, G.; Wang, H.; Perrault, A. R.; et al. Mechanisms of DNA Double Strand Break Repair and Chromosome Aberration Formation. *Cytogenet. Genome Res*. **2004**, *104*, 14–20.
33. Godschalk, R. W.; Ersson, C.; Riso, P.; et al. DNA-Repair Measurements by Use of the Modified Comet Assay: An Inter-Laboratory Comparison within the European Comet Assay Validation Group (ECVAG). *Mutat. Res*. **2013**, *757*, 60–67.
34. Chen, Y.; Li, Z.; Dong, Z.; et al. 14-3-3sigma Contributes to Radioresistance by Regulating DNA Repair and Cell Cycle via PARP1 and CHK2. *Mol. Cancer Res*. **2017**, *15*, 418–428.
35. Mohammad, D. H.; Yaffe, M. B. 14-3-3 Proteins, FHA Domains and BRCT Domains in the DNA Damage Response. *DNA Repair (Amst.)* **2009**, *8*, 1009–1017.
36. Harvey, K. F.; Zhang, X.; Thomas, D. M. The Hippo Pathway and Human Cancer. *Nat. Rev. Cancer* **2013**, *13*, 246–257.
37. Xu, T.; Wang, W.; Zhang, S.; et al. Identifying Tumor Suppressors in Genetic Mosaics: The *Drosophila lats* Gene Encodes a Putative Protein Kinase. *Development* **1995**, *121*, 1053–1063.
38. Morley, N.; Rapp, A.; Dittmar, H.; et al. UVA-Induced Apoptosis Studied by the New apo/necro-Comet-Assay Which Distinguishes Viable, Apoptotic and Necrotic Cells. *Mutagenesis* **2006**, *21*, 105–114.
39. Fairbairn, D. W.; Walburger, D. K.; Fairbairn, J. J.; et al. Key Morphologic Changes and DNA Strand Breaks in Human Lymphoid Cells: Discriminating Apoptosis from Necrosis. *Scanning* **1996**, *18*, 407–416.
40. Kizilian, N.; Wilkins, R. C.; Reinhardt, P.; et al. Silver-Stained Comet Assay for Detection of Apoptosis. *Biotechniques* **1999**, *27*, 926–930.
41. Bonse, J.; Wennmann, D. O.; Kremerskothen, J.; et al. Nuclear YAP Localization as a Key Regulator of Podocyte Function. *Cell Death Dis*. **2018**, *9*, 850.
42. Tranchant, R.; Quetel, L.; Tallet, A.; et al. Co-Occurring Mutations of Tumor Suppressor Genes, LATS2 and NF2, in Malignant Pleural Mesothelioma. *Clin. Cancer Res*. **2017**, *23*, 3191–3202.
43. Okada, N.; Yabuta, N.; Suzuki, H.; et al. A Novel Chk1/2-Lats2-14-3-3 Signaling Pathway Regulates P-Body Formation in Response to UV Damage. *J. Cell Sci*. **2011**, *124*, 57–67.
44. Zhao, B.; Tumaneng, K.; Guan, K. L. The Hippo Pathway in Organ Size Control, Tissue Regeneration and Stem Cell Self-Renewal. *Nat. Cell Biol*. **2011**, *13*, 877–883.
45. Yu, F. X.; Guan, K. L. The Hippo Pathway: Regulators and Regulations. *Genes Dev*. **2013**, *27*, 355–371.
46. Wang, Y.; Xu, X.; Maglic, D.; et al. Comprehensive Molecular Characterization of the Hippo Signaling Pathway in Cancer. *Cell Rep*. **2018**, *25*, 1304–1317.e5.
47. Reuven, N.; Adler, J.; Meltser, V.; et al. The Hippo Pathway Kinase Lats2 Prevents DNA Damage-Induced Apoptosis through Inhibition of the Tyrosine Kinase c-Abl. *Cell Death Differ*. **2013**, *20*, 1330–1340.
48. Collins, A. R.; Dusinska, M.; Horska, A. Detection of Alkylation Damage in Human Lymphocyte DNA with the Comet Assay. *Acta Biochim. Pol*. **2001**, *48*, 611–614.
49. Collins, A. R. The Use of Bacterial Repair Endonucleases in the Comet Assay. *Methods Mol. Biol*. **2017**, *1641*, 173–184.
50. Townsend, T. A.; Parrish, M. C.; Engelward, B. P.; et al. The Development and Validation of EpiComet-Chip, a Modified High-Throughput Comet Assay for the Assessment of DNA Methylation Status. *Environ. Mol. Mutagen* **2017**, *58*, 508–521.
51. Ngo, L. P.; Chan, T. K.; Ge, J.; et al. Microcolony Size Distribution Assay Enables High-Throughput Cell Survival Quantitation. *Cell Rep*. **2019**, *26*, 1668–1678.e4.